ELSEVIER

Journal of Nuclear Materials 266–269 (1999) 986–992

journal of nuclear materials

Non-uniform carbon redeposition on graphite

P. Wienhold [a,*], F. Weschenfelder [a], P. Karduck [b], K. Ohya [c], S. Richter [b], M. Rubel [d], J. von Seggern [a]

[a] *Institut für Plasmaphysik, Forschungszentrum Jülich GmbH, EURATOM Association, Trilateral Euregio Cluster, D-52425 Jülich, Germany*

[b] *Central Facility for Electron Microscopy, Aachen University of Technology, D-52056 Aachen, Germany*

[c] *Faculty of Engineering, The University of Tokushima, Tokushima 770, Japan*

[d] *Alfvén Laboratory, KTH Stockholm, Ass. EURATOM-NFR, S-10405 Stockholm, Sweden*

Abstract

Gradual erosion of a thin a-B:D layer on a graphite block is observed in TEXTOR-94 during 28 exposures while carbon out of the SOL has been deposited onto the surface simultaneously. The co-existence of B erosion (−0.5 nm/s) and C deposition (+0.8 nm/s) in the same area is due to non-uniform carbon redeposition of typically 10–30 μm in size. The D content is more than doubled in the co-deposit despite the considerable erosion of boron. Erosion by only neutrals could be discriminated from the erosion by D^+ ions. The film lost the transparency due to temperature excursions up to 2000 K during NBI. Observations were made during the exposures (colorimetry, spectroscopy) and post-mortem.

Keywords: In situ erosion/deposition measurement; Boronized graphite; Carbon deposition; Surface roughness; Scrape-off layer; TEXTOR

1. Introduction

Since graphitic material is a candidate for parts of the wall of ITER the control of carbon erosion and redeposition is a major concern. The built-up of carbonaceous layers by co-deposition with hydrogen does not only affect the tritium content [1], but may also end in the formation of carbon flakes or dust [2] which are difficult to remove out of the machine [3]. The change of the composition due to implanted carbon can prolong the life time of protecting coatings. This was suggested by observations made in a time resolved manner when a boron film became eroded under simultaneous carbon ion influx in the scrape-off layer (SOL) of TEXTOR-94 [4]. However, the experiment left open the question how the boron film became further eroded while the carbon deposit on top of the film had already reached thicknesses much higher than implantation depth. This finding is hardly to understand in an image which assumes that redeposits cover the surface as closed and uniform film. Non-uniform surface coverage, however, could very well explain that in net deposition zones the erosion continues from the still uncovered areas. Such a possibility has been mentioned [5] already when continual erosion of beryllium was found in a carbon net deposition zone. The erosion experiment described in the following aimed therefore mainly to clearly identify the non-uniformity of carbon net deposition and to determine a characteristic size of the formed carbon ''islands''. Average rates for the simultaneous boron erosion and carbon deposition are given and related to the deuterium ion fluxes. The uptake of additional deuterium by the carbon redeposit could be quantified as well as erosion in areas shadowed from the ions. Although we do not have a final answer to the question whether the surface roughness or other experimental circumstances like temperature excursion trigger non-uniform carbon redeposition it can not be excluded that this phenomenon acts as a precursor for flaking.

* Corresponding author. Tel.: +49 2461 61 3203; fax: +49 2461 61 2660; e-mail: p.wienhold@fz-juelich.de

0022-3115/99/$ – see front matter
PII: S0022-3115(98)00626-6

2. Experimental

A graphite block (60 × 63 mm) was inserted into the SOL of TEXTOR-94 (section 10/11) from the bottom with its upper plane surface declined by 29.5° to the toroidal field direction and oriented to the ion drift side. This surface was pre-boronized and covered by a thin and transparent a-B:D film to be eroded. An aluminum interlayer (≈180 nm) separated the film from the graphite matrix. Because of the tilting each point on the surface corresponded to another radial distance from the plasma center. It ranged from 46.6 to 50.2 cm (plasma radius $r_a = 46$ cm). Aluminum plates (1 mm) covered the block, avoided carbon sputtering and direct contamination of the surface. A thick Al-shield kept virgin also part of the boron film, but created with its upper edge (ending 2 mm above the tilted surface) a small shadow of 3.5 mm with respect to the toroidal direction. This became well visible (Fig. 1) after the exposure to 28 discharges (178 s total exposure time, $n_{eo} = 2.5 \times 10^{13}$ cm^{-3}, $T_{eo} = 1$ keV, $I_p = 350$ kA, $B_T = 2.25$ T), most of them additionally heated by neutral beam co-injection (NBI) with 1.3 MW for 2 s.

Fig. 1 shows the tilted sample with the four screw holes in top view. The left edge corresponds to $r = 50.2$ cm and the right to 46.6 cm. Before exposure, the initial a-B:D film appeared in the 2nd order interference colours (left) which indicates a thickness variation between about 165 nm (purple) and 230 nm (green-yellow) if the optical constants $n = 2.3$ and $k = 0.13$ measured by ellipsometry are assumed. Thereafter (right), only the protected left edge showed the original interference colour (purple) which in the adjacent strip of the shadowed region changed to dark yellow (145 nm). The insert shows the plasma near edge of the sample radiating in its own light 20 ms after terminating a NBI pulse. The temperature exceeded 2000 K as has been determined colorimetrically. It levels off to liner temperature (250°C) within 2–3 cm distance. Film and deposit in the central part of the sample were strongly affected and gradually transformed into a non-transparent material of greyish appearance.

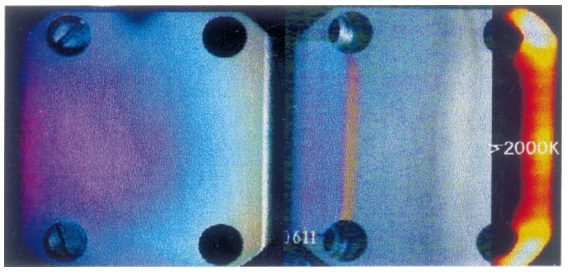

Fig. 1. Top view onto the tilted sample with the four screw holes before the experiment (left) and after (right). The colors are of 2nd interference order. The insert shows the plasma near edge radiating 20 ms after terminating NBI.

Plasma edge densities and temperatures were measured by the Li- and He-beam diagnostics [6] and determined for the ohmic phase of the discharges to typically $n_e(r_a) = 1.7 \times 10^{12}$ cm^{-3} ($\lambda_e = 2.4$ cm) and $T_e(r_a) = 48$ eV ($\lambda_T \approx 10$ cm), increasing during the NBI phase to $n_e(r_a) = 2.1 \times 10^{12}$ cm^{-3} ($\lambda_e = 2.7$ cm) and $T_e(r_a) = 60$ eV ($\lambda_T \approx 6$ cm). This rises the ion flux from $\Gamma_{D^+}(r_a) \approx 1.1 \times 10^{19}$ cm^{-2} s^{-1} ($\lambda \approx 2.1$ cm) to $\Gamma_{D^+}(r_a) \approx 2.3 \times 10^{19}$ cm^{-2} s^{-1} ($\lambda \approx 2.2$ cm). Since the ion temperatures $T_i(r_a) \approx 240$ eV were found to be four times T_e during the NBH phase [7] the estimated heat load exceeded 1100 W/cm^2 at the edge of the sample. This can explain rather well the temperature excursion. Note, that the values of the fluxes hitting the declined surface have to be weighed by sin 29.5°.

3. Observations during the exposure

3.1. Colorimetry

This technique [8] determines thickness distributions of thin transparent films from their interference colour pattern in illuminating light. Images were taken after each of the plasma discharges and line scans created along the center line in toroidal direction. Poloidally is almost no change. Fig. 2 shows few examples, which demonstrate the succeeding erosion of the boron film with time. Drastic erosion is observed at the plasma near edge of the sample. Here, the initial film of 230 nm (squares) vanished in less than 33 s (triangles) corresponding to rates of 7–9 nm/s. Although the film lost gradually its transparency so that the profiles could not

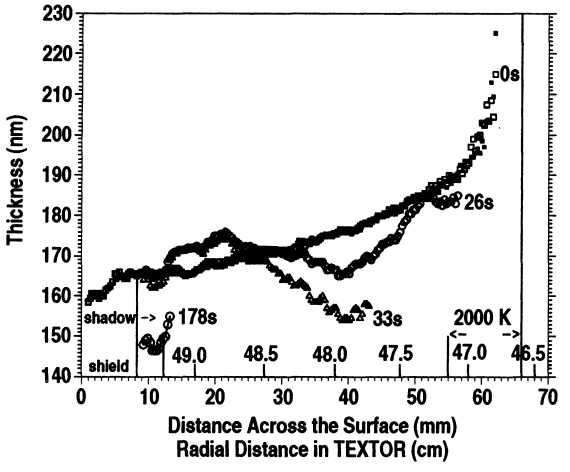

Fig. 2. Examples of thickness profiles along the centerline of the sample as measured by colorimetry. Times elapsed are given as well as radial distances from the plasma center.

further be determined, its almost full erosion could be stated from the naked Al-interlayer and from the later post-mortem analyses. This rate is higher than expected from the upper mentioned ion fluxes which can erode only ≈150 nm in 33 s if a sputter yield $Y = 0.01$ [9,10] and the ratio 2:1 for ohmic to NBI phase are taken into account and a density $\rho \approx 1 \times 10^{23}$ cm^{-3} for a-B:D [11] is assumed. It is likely, however, that great part of the boron has simply been evaporated (cf. 4.1).

The central part of the surface could not be observed doubtfree by colorimetry because of the progressive transformation of the film into a non-transparent phase. But in the shadow region of the upper Al-shield measurements were easy possible. As an example, the last determined thickness profile (circles, 178 s) is given. Although at $r \approx 49.5$ cm the parallel ion fluxes are lowered to only 1/3 ($\approx 3 \times 10^{18}$ cm^{-2} s^{-1}) the observed erosion rates have dropped here by a factor >50 to 0.1–0.2 nm/s. Provided $Y = 0.01$ this suggests an accordingly lower eroding flux $\Gamma_o \approx 1.7 \times 10^{17}$ cm^{-2} s^{-1} of most likely neutrals, because the ions are shielded (gyroradii <1 mm for 240 eV). Neutral fluxes of about 3×10^{16} cm^{-2} s^{-1} can be expected in TEXTOR at $r = 49.5$ cm in ohmic discharges [12] and might increase during NBI. But, they can become much higher near a solid surface due to the hydrogen recycling in form of molecules and their following dissociation [13] in the SOL. No carbon deposition had to be taken into account in the shadowed area as became obvious by means of sputter Auger electron analysis (AES) depth profiling. Such a perfect shadowing indicates charge states of 3 or 4 of the carbon ions (gyroradii below 1 mm).

3.2. Spectroscopy

The distributions of the BII and CII line emission above the surface have been recorded in side view by means of a CCD camera during various discharges. Maximum intensity was detected along lines parallel to the last close flux surface (LCFS) at $r = 46.4$ cm (BII) and 46.3 cm (CII) in spite of the tilting of the probe. This indicates the particles eroded or reflected from the surface which approach the first ionisation few mm adjacent the LCFS. The ionisation probability does not seem to be significantly different for boron or carbon. But, as Fig. 3 shows, the distribution of the BII light is peaked near the probes tip where the eroding fluxes are highest. The CII distribution can be much broader if we assume that carbon out of the background is deposited and re-eroded from the whole surface. It covers the boron in net deposition zones and protects it from further erosion. This, however, cannot explain why the absolute values of the BII light intensities do almost not change throughout experiment (178 s). The fluxes at e.g. $r =$ 47.5 cm could erode more than 500 nm in such a time

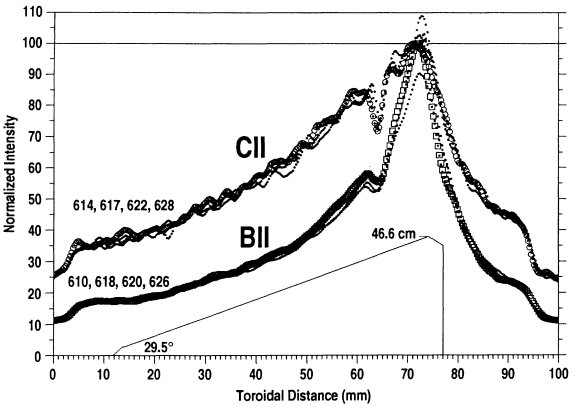

Fig. 3. Maximum intensities of the CII and BII light emission measured parallel to the LCFS during NBI. The distributions do not change with exposure time and are normalized for #617 (CII) and #618 (BII) only.

and simply erase the boron film. This is obviously not the case and points into the direction that carbon hinders boron erosion, but does not perfectly protect it. Note, that Fig. 3 presents the traces in the measured relations, only traces #617 (CII) and #618 (BII) are normalised to 100 in the maximum.

4. Investigations after exposure

4.1. Nuclear Reaction Analysis (NRA)

Boron and deuterium areal concentrations across the surface were determined by the nuclear reactions with beams of protons (640 keV) and ^{3}He (770 keV), respectively. The carbon deposits on the Al-shields were investigated by proton resonance backscattering of ^{12}C.

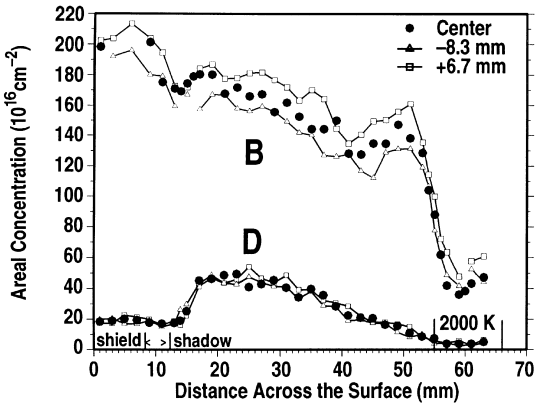

Fig. 4. Boron and deuterium concentrations along centerline and parallel to it as measured by nuclear reaction analysis (NRA).

Fig. 4 shows three parallel line scans taken in the central part of the sample which do not significantly differ. The initial boron concentrations (shielded area) drop somewhat (≈15%) in the shadowed region as was found already by colorimetry (3.1). The further decrease is less steep and rather irregular with a space resolution not sufficient to interpret details. Obviously, considerable amounts of boron are still present on the surface to feed further liberation. Since the eroding fluxes are sufficient to deplete the boron, approximately 400 nm of carbon can be estimated to be deposited and simultaneously reeroded at e.g. $r = 47.5$ cm in order to keep the balance. It would correspond to a flux of $\Gamma_C \approx 3 \times 10^{16}$ cm^{-2} s^{-1} of C ions if reflection is neglected. This estimate is a lower limit, however, because the implantation and deposition of carbon will increase the value of Y. The analysis of the carbon deposited on top of the Al-shield ($r = 49.5$ cm) results into a flux of $\approx 1.5 \times 10^{16}$ cm^{-2} s^{-1} which fits a decay length of $\lambda_C \approx 3$ cm [14]. At the hot edge (2000 K) the sudden drop of the boron concentration is likely due to evaporation because the fluxes do not change abruptly. Since the initial thickness profile went up (cf. Fig. 2) the boron loss is even more remarkable. Nevertheless, small boron amounts (≈50 nm) remained after the thermal impact possibly in the form of carbides. It could not be clarified, however, whether titanium impurities present below the Al-interlayer played a role.

Deuterium (lower curves) was found with a ratio D/B = 0.1 in the shielded area. This low value is expected because of the high sample temperature (250°C) during boronisation [15] which did not exceed during the experiment. No change is observed in the shadow region, but out of it a sudden increase up to a factor of 2.5 despite the drastic loss of boron. This indicates the net deposition of a-C:D which can exist with higher D-contents at the same temperature [16]. Approaching the hot zone the content decreases by thermal desorption due to the heat wave and levels off at 2000 K.

4.2. Depth profiling by sputter Auger electron analysis

Carbon was indeed found by AES to be deposited all over the surface except in the shielded and shadowed area. Only one characteristic example taken well in the deposition zone (23 mm distant from the shielded edge; $r = 48.8$ cm) can be given here. Fig. 5 seems to indicate carbon net deposition of ≈110 nm on top of a boron film with about 150 nm thickness if the intersections of the profiles are interpreted as interfaces. This is not unlikely because the virgin film was only 170 nm thick (cf. Fig. 2) and NRA yields a loss of 25 nm. But, it is surprising that the interfaces between C, B and Al range over the total depth. In particular the carbon implantation can affect only the first 15 nm. As an example one quasi-stationary implantation profile

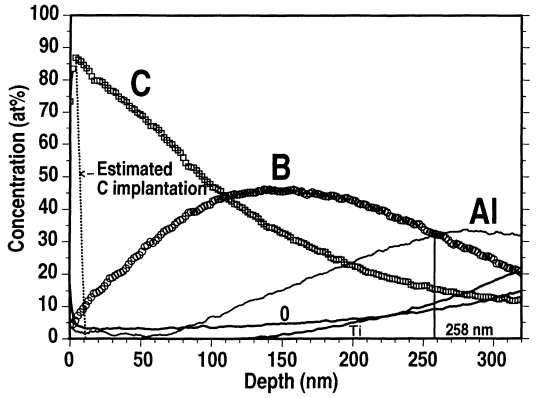

Fig. 5. Sputter AES depth profiles of C, B, Al, O in deposition zone 1. The implantation profile estimated for C^{4+} is also given (dots). Ti is impurity below the Al-interlayer.

[17] calculated for C^{4+} and for similar experimental conditions is dotted into the figure. It hardly explains the presence of carbon deep in the boron matrix or the appearance of boron near the carbon surface. According to investigations of the Al-shields for boron the fluxes in the SOL can be neglected as a source. Obviously, the profiles do not reflect the dependence of the elemental composition on depth, but rather the influence of the imperfection of the graphite substrate which consists of grains (2–4 μm) much thicker than the film (few 100 nm). With a spot size of the probing beam estimated to be about 5 μm it remained unclear, however, why a carbon film of 110 nm thickness should not better be discriminated. But, if carbon is non-uniformly deposited leaving part of the surface open it can very well be that C and B from neighboured areas are detected simultaneously and cause the measured broad transitions.

4.3. Electron probe micro-analysis (EPMA)

This technique determines the areal concentrations of the chemical elements in the film from their characteristic X-ray intensities excited by a 7 keV electron beam. The energy is too small in order to penetrate the Al-interlayer. To measure the aluminum thickness a beam energy of 20 keV has been used. Fig. 6 shows line scans taken every 0.5 mm along the center line across the sample. Aluminum (crosses) is still rather uniformly distributed over the surface with areal concentrations corresponding to 180 nm thickness except near the hot end where most of it seemed to be evaporated. The remnants may exist in form of stable compounds with B and C.

The values for the boron film (light bars) laying on top of the Al are also rather uniformly distributed in the shielded and shadowed area. The drop by about 20%

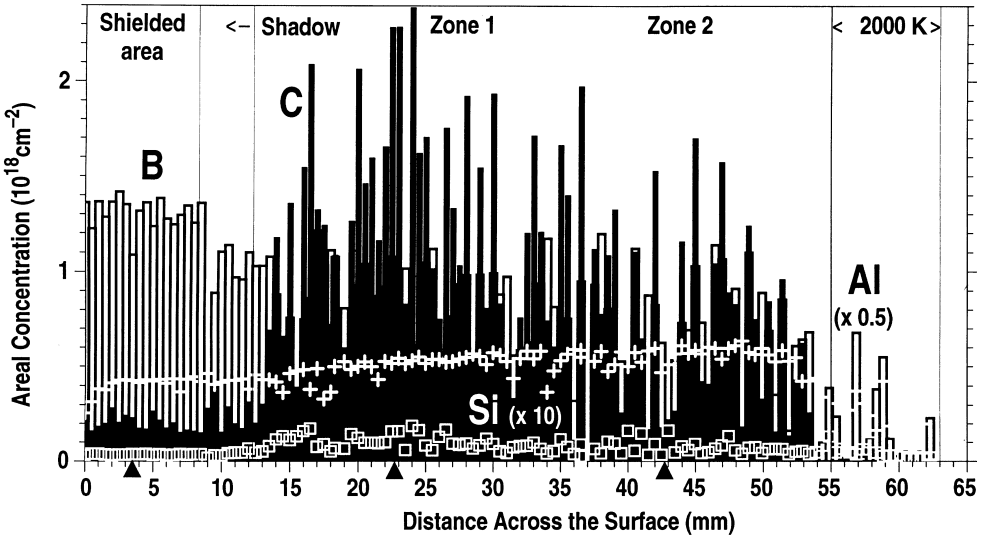

Fig. 6. Areal concentrations of B, C, Al, Si measured by electron probe micro-analysis (EPMA) in steps of 0.5 mm along centerline.

confirms the result found by NRA. Also the further distribution follows the irregular trend already observed by NRA. The systematic deviation of about 30% between the two techniques is not yet fully understood, but is probably due to the different sizes of the probing beams (mm for NRA, μm for EPMA). This will, however, not play a role in the further discussion. Some carbon (≈10%) is present already in the virgin boron film. It has been confirmed by AES sputter analysis of a Si-sample boronised together with the probe and will be taken into account in the later discussion. The value does not change in the shadow region. But, on the rest of the surface that was exposed to the SOL-plasma are deposited considerable amounts of carbon (black bars). Although the values tend to decrease against the plasma near end of the sample the distribution of the carbon is extremely non-uniform. Concentrations up to 2×10^{18} cm^{-2} corresponding to about 300 nm are directly neighboured by almost no deposition. Correlation analysis showed that this carbon is clearly related with the co-deposited silicon impurities out of the SOL, but not with the boron. The curve (squares) shall give an impression of the quantities only.

Doubtless, the coverage is a net effect of the combined carbon deposition and erosion due to deuterium ions. In spite of fluxes which can erode 500 nm and more the average thickness of carbon has grown to about 125 nm. At the same time (178 s) the boron film became roughly 100 nm thinner. Continuous C deposition simultaneously existing with continuous B erosion strongly suggests the non-uniformity of the carbon distribution on the area. The space resolution of 0.5 mm for the single measurements is not sufficient, however, to determine characteristic sizes. EPMA analyses every 5 μm with a spot size of 2–3 μm have been done therefore at three selected 1 mm wide spots (triangles below the abscissa) at a distance 3 mm from the edge (shielded area), 22 mm (deposition zone 1), and 42 mm (deposition zone 2). Only one result (deposition zone 2) can be given here (Fig. 7).

Basically, the higher space resolved distribution shows similar appearance as before. Locations with areal concentrations up to 2×10^{18} cm^{-2} are neighboured by almost no carbon, but now on a scale counting in μm. This indicates non-uniform deposition. The characteristic size seems to be 10–30 μm. The extreme data scatter of 70% with an average of 9.3×10^{17} cm^{-2} is much larger than the data scatter due to the surface topography. The scatter expected due to the topography is ±20% only as has been determined in the shielded area which remained uniform. The boron distribution is similar irregular, because its non-uniform protection causes non-uniform erosion. The average is now 73 nm (±40%) instead of 175 nm at the beginning, but still locations exist of uncovered boron which can be eroded. The average values correspond to erosion rates of −0.57 nm/s for B and deposition rates of +0.63 nm/s for C if the background is subtracted and a density of 6.5×10^{22} cm^{-3} for a-C:D is assumed [14]. Because of the slow total growth rate the surface will likely be depleted from boron in a long run. Net erosion was found in earlier experiments [4] in zones $r >$ 48.4 cm. In deposition zone 1 the analysis yielded more different rates of −0.4 nm/s for B and of +1.0 nm/s for C and a rather closed carbon coverage after the 178 s total exposure time. But, also here the boron film had been eroded before differentially to an average thickness of 83 nm.

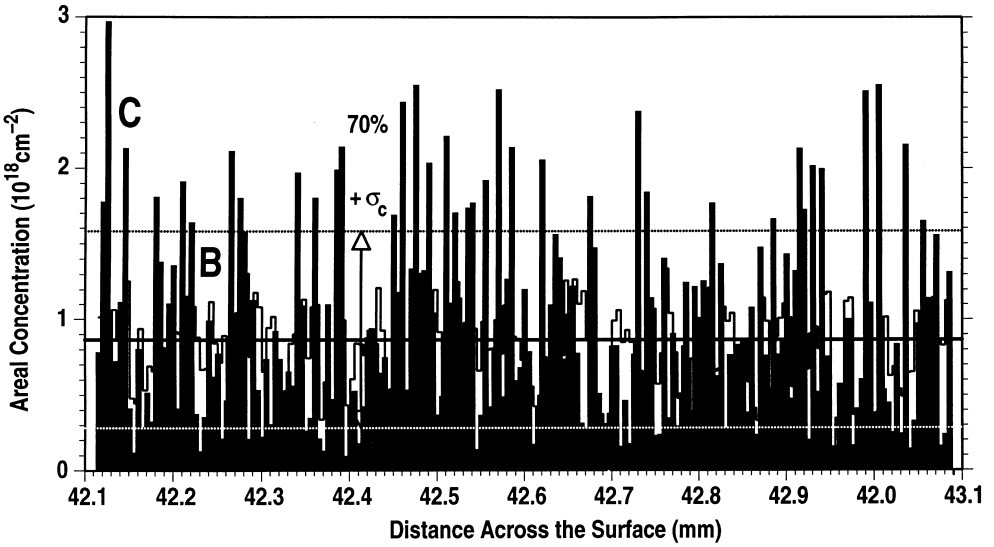

Fig. 7. EPMA for B and C in deposition zone 2 with high space resolution of 5 μm. The spot size of the probing beam is 2–3 μm.

4.4. Wavelength dispersive X-ray mapping

The two-dimensional distributions of B and C in surface areas of 65 μm × 65 μm were determined from the K_α-light excited by an electron beam of 7 keV scanned over the surface (resolution of 256 × 256 pixel). As EPMA, this energy yields information depths until the Al-interlayer, but with not calibrated intensities. The cut-off for noise was set to the median value of the total intensity distribution. In the shielded area the rather uniform boron coverage could be confirmed. The distributions are very irregular, however, in deposition zone 1 (Fig. 8). The red colour represents areas where only carbon is detected. Boron has already been eroded here. In the blue coloured zones both of the species commonly exist. But there are still areas with only boron (green) without carbon deposition. Few spots remained empty (black). The pattern depends on the definition of the cut-off intensity, but other attempts made did not change the major conclusion that the carbon seemed to form irregular shaped islands. Great care was taken in order to rule out errors due to surface roughness. Investigations made with atomic force microscopy (AFM) (not shown, see e.g. [18]) revealed a roughness of few tenths of a μm due to the grains which do not affect the signal intensity. Grooves likely caused by polishing were found to be 1–1.5 μm deep at distances of 15–20 μm. This value seems to coincide with the typical size of the non-uniform carbon coverage and coincides also with the typical dimension of the microstructure in carbon flakes found recently in TEXTOR [19]. It is rather unclear, however, how the surface topography can trigger carbon agglomeration. Other processes like temperature enhanced mobility on the surface above 1700°C could result into a turbostratic growths of pyrolytic carbon [20] on the affected areas. It remains speculation, whether the observed non-uniformity of the deposits could act as precursors for flaking until the forthcoming experiments are evaluated.

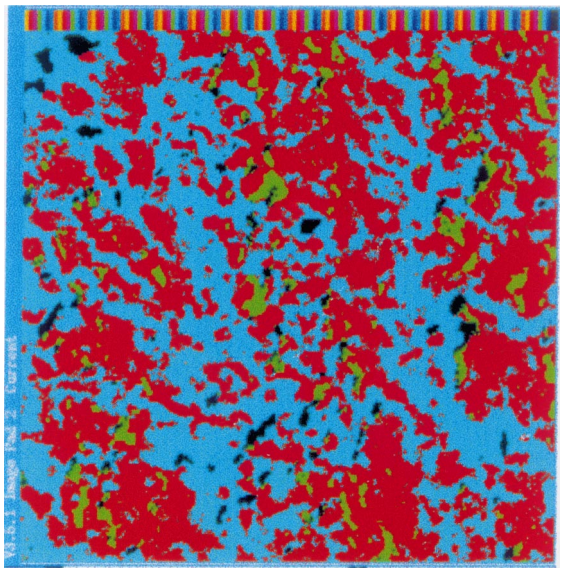

Fig. 8. Distribution of carbon and boron in an area of 65 μm × 65 μm as found by wavelength dispersive X-ray mapping (WDX) in deposition zone 1; red: carbon only, no boron; blue: carbon as well as boron; green: boron only, no carbon; black: no signal.

5. Conclusions

The major conclusion we draw from the observations is that the erosion of the boron film by hydrogen ions can happen simultaneously with a carbon deposition out of the background plasma up to thicknesses much higher than implantation depth. Reason is the non-uniformity of the carbon deposition which does not perfectly protect the boron surface and allows further and according non-uniform erosion. The phenomenon of differential erosion makes it more complex to consider net erosion or deposition as being independent on the surface location. With average rates of about +0.8 nm/s for C and −0.5 nm/s for B the carbon thickness can grow to 300 nm while the neighboured boron loses 100 nm. Characteristic for the islands are irregular shape and sizes of 10–30 μm which is in the order of the microstructure of the carbon flakes. Whether surface topography or temperature excursion can cause the non-uniformity and the agglomeration of carbon has to be clarified by further experiments. Because of the increased lifetime of the film boron remains longer active as getter for oxygen impurities in the machine. This benefit is on the cost of a growing tritium reservoir due to the carbon deposit, both relevant for ITER. Despite boron erosion the deuterium content was found to be increased by more than a factor of 2 in the carbon deposition zone compared to the virgin a-B:D.

The fluxes in the SOL estimated from measured densities and temperatures for electrons and ions fit well into the observed erosion/deposition rates and can rather explain the observed temperature excursion of 2000 K at the plasma near edge of the sample. Most of the initial boron (≈200 nm) and of the aluminum interlayer (≈180 nm) are evaporated, but remnants still exist (≈50 nm) probably in the form of carbides more stable against erosion than a-C/B:D. In an area shadowed from the ions (D^+, C^{4+}) erosion by only neutrals is observed with fluxes considerably higher than in the SOL and most likely caused by hydrogen recycling from the surface. This possibly yields experimental access to better model hydrogen recycling processes on a solid surface.

Acknowledgements

The authors like to thank A. Aretz for the AFM studies, M. Brix and H. Huber for evaluating the SOL data, and F. Römer for the preparation of the Al-interlayer. We had technical assistance by M. Freisinger and H. Reimer, and the TEXTOR team.

References

[1] G. Federici, D. Holland, G. Janeschitz, C.H. Wu, J. Nucl. Mater. 241–241 (1997) 260.
[2] J. Winter, 24th EPS Conf. on Contr. Fusion and Plasma Physics, Berchtesgaden, Germany, 9–13 June 1997.
[3] V. Philipps, H.G. Esser, J. von Seggern, H. Reimer, M. Freisinger, E. Vietzke, P. Wienhold, these Proceedings.
[4] P. Wienhold, F. Weschenfelder, J. von Seggern, B. Emmoth, H.G. Esser, P. Karduck, J. Winter, J. Nucl. Mater. 241–243 (1997) 804.
[5] D. G Whyte, J.N. Brooks, C.P.C. Wong, W.P. West, R. Bastasz, W.R. Wampler, J. Rubenstein, J. Nucl. Mater. 241–243 (1997) 660.
[6] B. Schweer, G. Mank, A. Pospieszczyk, B. Brosda, B. Pohlmeyer, J. Nucl. Mater. 196–198 (1992) 174.
[7] A. Huber, A. Pospieszczyk, D. Rüsbüldt, B. Unterberg, German Physical Society Meeting, Bayreuth, Germany, to be published.
[8] P. Wienhold, F. Weschenfelder, J. Winter, Nucl. Instrum. Meth. B 94 (1994) 503.
[9] E. Vietzke, V. Philipps, K. Flaskamp et al., 10th Int. Symp. On Plasma Chem., Bochum, Germany, 4–9 August 1991.
[10] H. Toyoda, T. Isozumi, H. Sugai, T. Okuda, J. Nucl. Mater. 162–164 (1989) 732.
[11] A. Annen, R. Beckmann, W. Jakob, J. Non-Cryst. Solids 209 (1997) 240.
[12] Ph. Mertens, M. Silz, J. Nucl. Mater. 241–243 (1997) 842.
[13] U. Samm, P. Bogen, H. Hartwig, E. Hintz, K. Höthker, Y.T. Lie, A. Pospieszczyk, D. Rüsbüldt, B. Schweer, Y.J. Yu, J. Nucl. Mater. 162–164 (1989) 24.
[14] P. Wienhold, F. Waelbroeck, H. Bergsåker, et al., J. Nucl. Mater. 162–164 (1989) 369.
[15] A. Annen, M. Saß, R. Beckmann, W. Jacob, Thin Solid Films 300 (1997) 101.
[16] A. Annen, thesis, Univ. Bayreuth, Germany, 1997.
[17] K. Ohya, J. Kawata, Jpn. J. Appl. Phys. Part 2, 36 (3A) (1997) 298.
[18] N. Almqvist, M. Rubel, P. Wienhold, S. Fredriksson, Thin Solid Films 270 (1995) 426.
[19] M. Rubel, J. von Seggern, P. Karduck, V. Philipps, A. Vevecka-Priftaj, these Proceedings.
[20] A. Oberlin, High resolution TEM studies of carbonization and graphitization, in: P.L. Walker, P.A. Thrower (Ed.), Chemistry and Physics of Carbon, vol. 22, Marcel Dekker, New York, 1990, p. 1.